

Article

Design and Analysis of a New Prefabricated Foundation for Onshore Wind Turbines

Xinyu Li ¹, Huageng Hao ², Haijun Wang ^{1,3}, Liying Zhang ², Yaohua Guo ^{1,3,*} , Jijian Lian ^{1,3,4}, Yanyi Du ⁵, Xianwen Wang ⁶ and Cong Zeng ⁷ 

¹ School of Civil Engineering, Tianjin University, Tianjin 300350, China; L_xinyu1@tju.edu.cn (X.L.); bookwhj@tju.edu.cn (H.W.); jjlian@tju.edu.cn (J.L.)

² China Huaneng Group Clean Energy Research Institute Co., Ltd., Beijing 102209, China; hk_hao@qny.chng.com.cn (H.H.); ly_zhang@qny.chng.com.cn (L.Z.)

³ State Key Laboratory of Hydraulic Engineering Intelligent Construction and Operation, Tianjin University, Tianjin 300350, China

⁴ Maritime College, Tianjin University of Technology, Tianjin 300384, China

⁵ Huaneng Longdong Energy Co., Ltd., Qingyang 745000, China; 18893605161@139.com

⁶ Huaneng Jilin Power Generation Co., Ltd., Jilin 130012, China; 15944995111@139.com

⁷ School of Civil Engineering and Architecture, Northeast Electric Power University, Jilin 132012, China; zc_1113@126.com

* Correspondence: guoyaohua@tju.edu.cn; Tel.: +86-182-2228-9536

Abstract: A new type of prefabricated foundation for onshore wind power was proposed in this paper. The stress and bearing mechanism of the new foundation was explored through theoretical calculation and finite element analysis. The results show that compared with the extended foundation in the same position, the amount of concrete in the new foundation is reduced by 30.00%, and the amount of rebars are reduced by 34.69%. The new prefabricated foundation has been inspected and calculated according to the specification. The calculation results indicate that the stress and initial reinforcement of the foundation meet the specification requirements. The bearing capacity, inclination rate, deformation, and stability of the foundation meet the requirements. Through finite element analysis, it is further confirmed that the structure meets the requirements of wind turbine operation, and the overall force meets the requirements of various indicators. The stress distribution of the foundation concrete and rebars is reasonable and uniform, and the load transfer is great. Also, the maximum stress of rebars and concrete does not exceed the specification limit, and the concrete remains intact without cracking or damage. The new foundation structural design and theoretical analysis were reasonable and accurate, and can be put into application in the future.

Keywords: onshore wind power; assembly; new prefabricated foundation; theoretical calculation; finite element analysis



Citation: Li, X.; Hao, H.; Wang, H.; Zhang, L.; Guo, Y.; Lian, J.; Du, Y.; Wang, X.; Zeng, C. Design and Analysis of a New Prefabricated Foundation for Onshore Wind Turbines. *Buildings* **2024**, *14*, 193. <https://doi.org/10.3390/buildings14010193>

Received: 17 November 2023

Revised: 7 January 2024

Accepted: 9 January 2024

Published: 12 January 2024



Copyright: © 2024 by the authors. Licensee MDPI, Basel, Switzerland. This article is an open access article distributed under the terms and conditions of the Creative Commons Attribution (CC BY) license (<https://creativecommons.org/licenses/by/4.0/>).

1. Introduction

At present, a new round of global energy and technological revolutions is in the ascendant. Vigorously developing renewable energy has become a major strategic direction for global energy transformation and the response to climate change. The global primary energy structure is rapidly moving towards diversification, cleanliness, and low carbon [1–4]. With the continuous growth of global energy transformation, wind power has developed rapidly and is poised to play a vital role in accelerating the global energy transition [5,6]. According to the Global Wind Report 2023 by the Global Wind Energy Council (GWEC), by the end of 2022, the cumulative installed capacity of global wind power reached 837 GW, of which onshore wind power was 780 GW and offshore wind power was 57 GW [6]. With more and more countries around the world developing the wind power business and wind power costs continuing to decline, the global wind energy industry will maintain a rapid development trend, and the global wind power installed

capacity will continue to grow. In 2022, 77.6 GW of new wind power capacity was added worldwide, of which the installed capacity of onshore wind power was 68.8 GW. The global wind energy market is expected to grow by 15% on average per year (Figure 1) [6]. Compared with offshore wind power, the development cost of onshore wind power is about a quarter of offshore wind power, and the operation and maintenance costs are also lower [7].

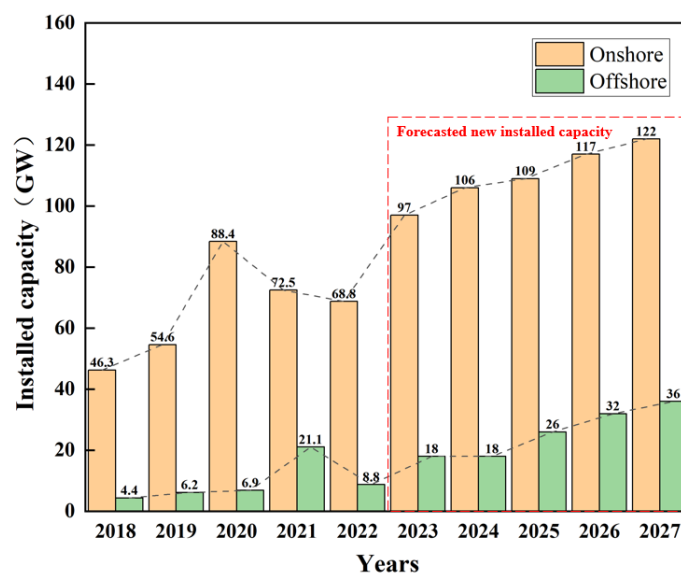


Figure 1. Global wind power capacity additions (GW) [6].

The continuous growth in overall energy demand and the related environmental impacts play a significant role in the large sustainable and green global energy transition [8–11]. The development mode and trend of wind power show the characteristics of gradual large-scale development and base construction, which puts forward higher requirements for the cost, construction period, and convenient installation of wind turbine foundations [12]. The traditional cast-in-place concrete construction technology is inefficient, polluting, and difficult to ensure quality, making it unsuitable for the high-quality development of the wind power industry [13–15]. Changing the traditional form of cast-in-place reinforced concrete foundations and developing efficient, economic, and green prefabricated foundations is the inevitable trend of economic construction and sustainable development in the new period. It has great potential and market benefits, and will improve the infrastructure [16,17]. The concept of assembled wind turbine foundations is in line with the development requirements of building industrialization. The assembled wind turbine foundation adopts the construction method of standardized design and factory mass production, and it can solve the quality and discontinuous pouring problems caused by on-site mixing in remote mountainous areas due to the non-transportation of commercial mixing. While effectively ensuring the quality of the foundation, it significantly shortens the construction period, saves consumables, reduces energy consumption, and minimizes environmental pollution, which is conducive to the early production and power generation of the wind turbine. It can be recycled after the service period [12,18–20].

Currently, the main structural forms of onshore wind power assembled foundations include the assembled box girder foundation, the assembled raft foundation, the assembled spread foundation, the assembled multi-footing foundation, the assembled braced foundation, and the assembled tubular foundation (Figure 2) [12]. RUTE Foundation Systems has developed a fully assembled box girder foundation. The beam is divided into three or more different box-type prefabricated components, and has strong flexibility in the design and construction of the foundation [21]. The assembled raft foundation of onshore wind power has the advantages of a clear force transmission path, easy division

of prefabricated components, and a small connection area. It is the mainstream form of onshore wind power assembled foundation. RWE proposed a square prefabricated raft foundation with prefabricated beams and plates, which is divided into four types of prefabricated modules [22]. ANKER has developed a variety of fully assembled raft foundation structures [23]. Wu Xiangguo proposed to divide the complete main body of the extended foundation into two types of prefabricated concrete members through modularizing the extended foundation [24]. RUTE Foundation Systems has developed a prefabricated multi-footing foundation with post-tensioned prestressed connections. There are three different beam end support methods, the structure can significantly decrease material and time costs, and the overall stability is good. However, the shear strength of the joint surface of the pillar and rib beam does not meet the requirements under certain working conditions [25,26]. Ma Renle proposed a prefabricated tubular foundation. It has been proved that the structure is simple, the construction speed is fast, the cost is low, and it has good bending resistance [27,28]. The onshore wind power assembly support foundation originates from the Spanish company ESTEYCO. The foundation consists of a base, support, central tube, and roof. Only the support structure is prefabricated, and the on-site engineering quantity is still large. Compared to the traditional cast-in-place foundation, the construction period is shorter [29].

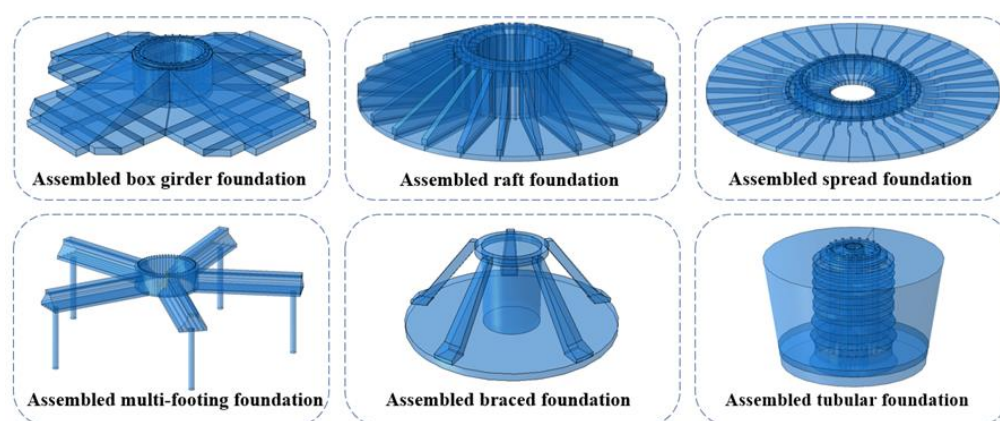


Figure 2. Main forms of assembled foundations for onshore wind turbines [21–28,30].

In this paper, we combined the mechanical characteristics of the existing assembled foundation structure with the advantages of raft foundation, taking into account the ease of transportation and construction. We proposed a new type of prefabricated foundation for onshore wind power to replace the existing raft foundation type, which effectively spreads the force and decreases the overall weight of the structure. It has certain advantages in transportation, economy, and hoisting. The main research contents of this paper are as follows: A new prefabricated foundation structure for onshore wind power was proposed, and its design and layout explained. The force and bearing mechanism of the new prefabricated foundation was explored through theoretical calculation and finite element analysis.

2. New Prefabricated Foundation for Onshore Wind Turbines

2.1. Foundation Structure

An onshore wind farm is situated in the hilly and gully area of Loess Plateau, with the ground elevation of the wind turbine ranging from 1763 to 1980 m. Most of the wind turbines in the field are located in the cultivated land formed through man-made transformation of loess beams, mound tops, or loess beams and mounds. The foundation form is mainly expansion foundation. In order to overcome the problems of a large engineering volume and complicated construction of the extended foundation, and combined with the structural form of prefabricated single-ribbed raft foundation (Figure 3), a new prefabricated assembled foundation is innovatively proposed in this paper. Compared to the single-ribbed raft foundation, the new prefabricated foundation integrates the prefabricated

girder slab foundation and the table pillar section as a whole, reducing the number and types of prefabricated components and improving construction efficiency.

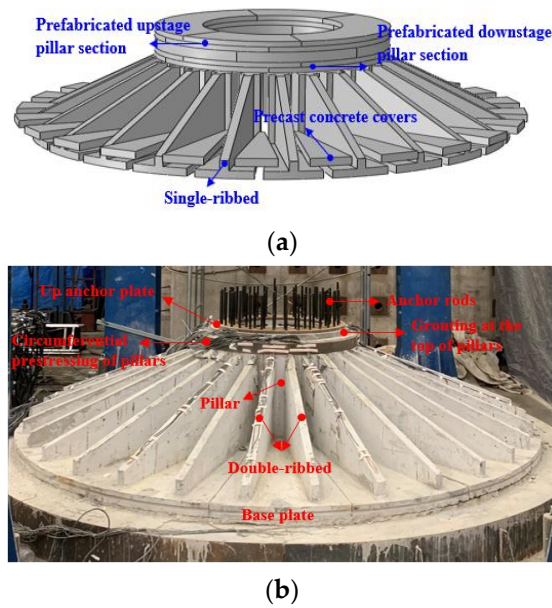


Figure 3. Comparison of preassembled raft foundation structures. (a) Single-ribbed raft foundation [23]. (b) Double-ribbed raft foundation (proposed in this paper).

The new prefabricated foundation consists of 16 blocks, and each block consists of two rib beams and a pillar. The diameter of the base is 21.6 m, the diameter of the pillar is 6.8 m, the thicknesses of the baseplate and rib beams are 0.4 m and 0.25 m, and the volume of one block is 22.55 m³. The structural form and dimensions are shown in Figure 4.

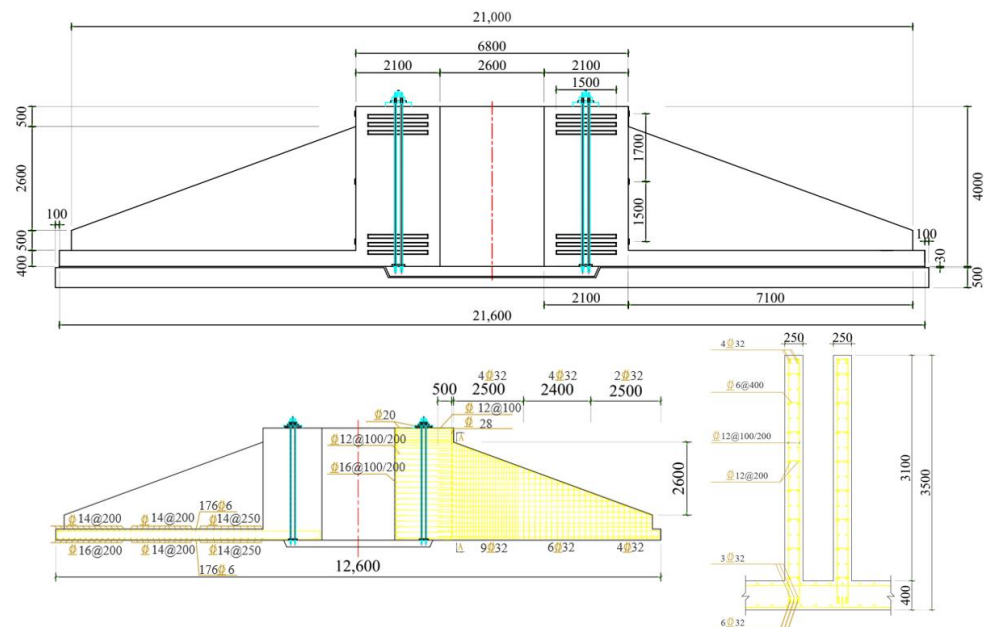


Figure 4. Foundation dimensions and schematic (units: mm).

The concrete consumption of one prefabricated foundation is approximately 360.84 m³ and 45.28 t of rebars. The typical circular extended foundation for this site is 3.5 m in height and 18 m in diameter, and is connected with the upper tower through prestressed anchors. The extended foundation at the same position requires approximately 515.47 m³ of

concrete and 52.46 t of rebars. The comparison of the two foundations in terms of material consumption is shown in Table 1. The new foundation reduces concrete by 30.00% and rebars by 13.69% compared with the extended foundation. Since the prefabricated blocks of the new foundation are fabricated in the factory and tested for quality before being sent to the site, the site only needs to be installed and spliced according to the requirements, so the construction efficiency and engineering quality of the new foundation are controllable and can be guaranteed.

Table 1. Comparison of two foundation materials.

Material Types	Extended Foundation	New Prefabricated Foundation	Reduce (%)
C40 concrete (m ³)	515.47	360.47	30.00
rebar (t)	52.46	45.28	13.69

The anchor bolt hole should be reserved in one single block, and the positioning and temporary internal support should prevent the displacement and deformation of the concrete during the pouring process. Before pouring the concrete, it is necessary to adjust the level and verticality of the anchor bolt hole and connect the new foundation with the up and down anchor plates through the anchor bolt. During the pouring process, continuous pouring should be carried out in layers without leaving construction joints, and the dimensions of each part of the component should be strictly controlled and uniformly accepted. The convex and concave shear keys between the pillars can be embedded with each other. The top, middle, and bottom layers of the pillars are equipped with six 1860-grade circumferential prestressed steel strands with a diameter of 15.2 mm. The six tension control stresses are 1280 MPa, and the ring anchors are fixed. The prestressed steel strands are protected with anti-corrosion grease and sheaths. The prestressed system should be tensioned in the order of middle-bottom-top layers. After tensioning the prefabricated block, the open space needs to be filled and repaired with high-level elevation concrete.

2.2. Construction Process of the New Prefabricated Foundation

The schematic diagram of each part of the structure is shown in Figure 5.

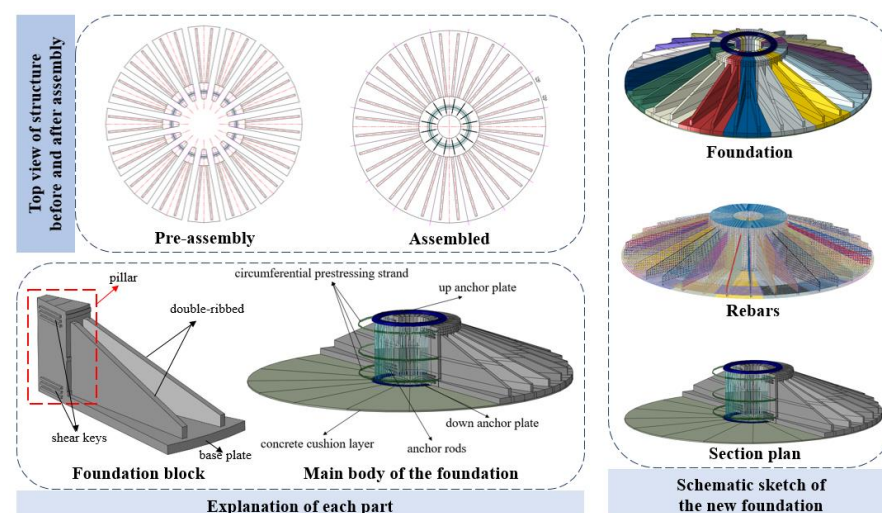


Figure 5. The schematic diagram of each part of the structure.

The construction process is shown in Figure 6: assembly of the new prefabricated foundation blocks, anchor rods connecting the up and down anchor plates with the foundation, grouting between pillars, prestressing tensioning, grouting on the top of the pillars, and anchor tensioning are performed in the sequence of operations.

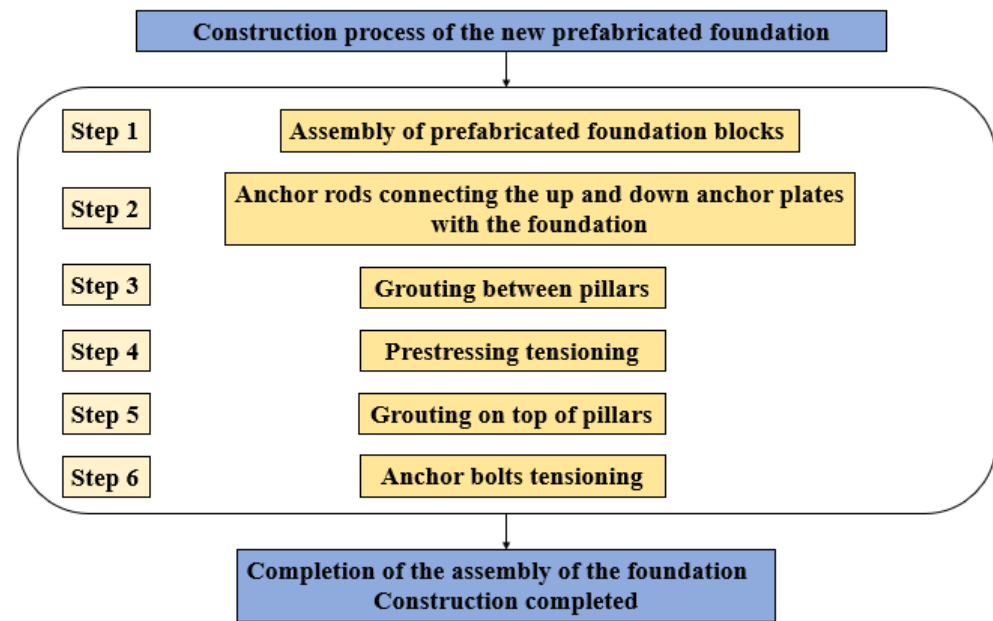


Figure 6. Construction process.

The 16 prefabricated blocks of the new foundation are positioned and placed, and embedded using shear keys for initial connection. Before grouting between pillars, each component needs to be connected and tightened using anchors. During the grouting process, it is important to check the fasteners. Before grouting, clean up the debris in the gap and pour the grouting between pillars. Then the anchors can be passed through the reserved circumferential holes. When the strength of the grouting material between the pillars reaches 80%, the tension of the circumferential prestressed system can be carried out to enhance the integrity of the foundation.

Finally, the up and down anchor plates and prefabricated foundation blocks are connected using anchors and bolts, grouting at the top of the pillars, and then tensioning the anchor bolts, which plays a positive role in the safety, stability, and durability of the later operation of the wind turbine.

In addition, the new foundation adopts large-scale intensive production, which can save consumables, and reduce energy consumption and construction waste to a certain extent. The new prefabricated foundation plate effectively solves the problems of a long construction period, slow construction speed, and difficult formwork support, and has the advantages of a simple structure and convenient installation. Its mechanized installation in the construction process can reduce air, noise, wastewater discharge, and other pollution, as well as reduce carbon emissions throughout the building's life cycle.

3. Theoretical Calculations

3.1. Wind Turbine Loads

The operating wind turbine is subjected to 360° loads and large eccentric forces, which will produce great loads on the tower and the foundation [31,32]. From the viewpoint of the structure system, wind turbines belong to structures with a "heavy head" [31]. The complex load on the top of the wind turbine is transmitted to the foundation top through the tower, and the load is transformed into horizontal load, vertical load, bending moment, and torque composite load. The wind turbine foundation GL coordinate system is shown in Figure 7.

The standard foundation load values for 4.20 MW wind turbines at an onshore wind farm were used for the calculation and analysis, as shown in Table 2.

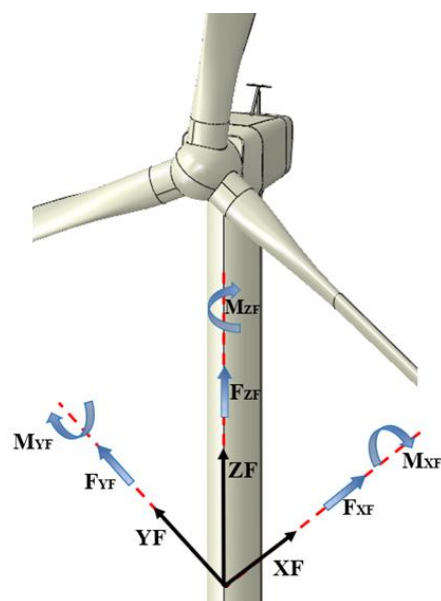


Figure 7. GL coordinate system of the wind turbine foundation [31].

Table 2. Standard values for wind turbine loads ($k_0 = 1.0$).

Loading Conditions	Wind Turbine Loads			
	Horizontal Load F_{xy} (kN)	Vertical Load F_z (kN)	Bending Moment M_{xy} (kN·m)	Torsion M_z (kN·m)
Normal operation of the wind turbine	626.979	4035	63,142.9	821.28
Extreme operation of the wind turbine	798.868	4029.39	83,612.3	743.42

Since the installed capacity of the wind turbine is 4.2 MW, greater than 2.5 MW, it meets the safety level of first-level infrastructure required by the specification. Therefore, when calculating the structure under the extreme operating conditions basic combination, it is necessary to take the structural importance coefficient into account. The specific load combination is shown in Table 3.

Table 3. Calculated load combinations for wind turbine foundations [33].

Conditions	Operational State	Load Combinations	Structural Importance Coefficient k_0
1	Normal operating loads	Standard combination	Disregard
2	Extreme loads	Standard combination	Disregard
3	Extreme loads	Basic combination	1.1

3.2. Theoretical Calculations

The design of a wind turbine foundation adopts the limit state design method so that the overall size meets the specification construction requirements, but also to carry out the foundation bearing capacity calculation, foundation stability calculation, rebars calculation of the foundation structure, material strength calculation, and crack width calculation [34].

3.2.1. Calculation of Structural Stability

The raft foundation mainly resists the deformation of the foundation through the stiffness of the beams and resists the overturning moment through the self-weight of the

filling between the foundation and the ribbed beams. The calculation method is similar to the design method of gravity-type extended foundation [33]. According to the *Code for Design of Wind Turbine Foundation for Onshore Wind Power Projects (NB/T 10311-2019)*, the calculation formulas of eccentric load on a circular foundation are as follows:

$$P_{k\max} = \frac{N_k + G_k}{A} + \frac{M_k}{W}, \quad (1)$$

$$P_{k\min} = \frac{N_k + G_k}{A} - \frac{M_k}{W}, \quad (2)$$

When calculated for the standard combination of normal load conditions, $P_{k\min} > 0$, the bottom surface of the foundation is not separated from the foundation. The characteristic value of the bearing capacity of the foundation bearing layer should be greater than 220 kPa. The actual bearing capacity of the surface foundation on site is about 153 kPa, and the foundation treatment is required.

Under the standard combination of extreme load conditions, $P_{k\min} < 0$, the bottom surface of the foundation is separated from the foundation, and the ratio of the base separation area is 3.49%. For the raft foundation, it is subjected to eccentric load outside the core area. The bottom surface of the foundation is partially separated, and the separation area is not more than 1/4 of the total area. The bottom pressure of the circular foundation of the wind turbine is calculated according to Formula (3), and the resulting bottom pressure of the foundation is 244.39 kPa.

$$P_{k\max} = \frac{N_k + G_k}{\zeta R^2}, \quad (3)$$

The anti-sliding force of the foundation bottom surface is calculated using Formula (4). Under the standard combination of normal operating load conditions, the anti-sliding force of the foundation bottom surface F_R is calculated as 12,536.95 kN. Under the standard combination of extreme load conditions, the foundation's bottom surface anti-sliding force F_R is 12,534.71 kN. The friction coefficient between the bottom of the foundation and the ground is 0.4 (the lower limit value) [35].

$$F_R = \mu \times N_k, \quad (4)$$

$$\frac{F_R}{\gamma_0 F_S} \geq \gamma_d, \quad (5)$$

The anti-sliding force and sliding force on the most dangerous sliding surface of anti-sliding stability should satisfy Formula (5). The ratios of F_R and F_S are 18.18 and 14.26, which are greater than the structural coefficient of 1.3 (γ_d). Therefore, the foundation's anti-slip stability meets the requirements.

The anti-overturning moment of the foundation should be calculated according to Formula (6). The foundation's anti-overturning moment is calculated to be 338,497.76 kN·m under the standard combination of normal operating load conditions. Under the standard combination of extreme load conditions, the foundation's anti-overturning moment is 338,437.17 kN·m. The anti-sliding force and sliding force on the most dangerous sliding surface of anti-sliding stability should meet Formula (7). The ratios of M_R and M_S are 4.68 and 3.54, which are greater than the structural coefficient of 1.6 (γ_d). Therefore, the foundation's anti-overturning stability meets the requirements.

$$M_R = N_k \times R, \quad (6)$$

$$\frac{M_R}{\gamma_0 M_S} \geq \gamma_d, \quad (7)$$

In calculating the foundation settlement deformation, the circular cross section of the foundation is equated to a rectangular cross section by area for ease of calculation, and its side length D is calculated as:

$$D = \sqrt{\frac{\pi d^2}{4}}, \quad (8)$$

where d is the diameter of the new prefabricated foundation, so the equivalent rectangular section side length D is 19.14 m. According to the *Code for Design of Wind Turbine Foundation for Onshore Wind Power Projects (NB/T 10311-2019)*, the settlement value can be calculated using the Formulas (9) and (10):

$$s = \psi_s s' = \psi_s \sum_{i=1}^n \frac{p_{0k}}{E_{si}} (z_i \bar{\alpha}_i - z_{i-1} \bar{\alpha}_{i-1}), \quad (9)$$

$$p_{0k} = \frac{F_{zk} + G_k}{A_s}, \quad (10)$$

The additional stress P_{0k} at the base of the foundation is calculated to be 86.77 kPa. The empirical coefficient of pile settlement ψ_s at this point is calculated to be 0.99 through linear interpolation, resulting in a final settlement deformation s of 42.04 mm for the foundation. The tower height of the designed wind turbine is 107 m. According to the *Design Code for Wind Turbine Foundations for Onshore Wind Farm Engineering (NB/T 10311-2019)*, the allowable value of foundation settlement is 100 mm when $90 \text{ m} < H \leq 120 \text{ m}$. The foundation's settlement is 42.04 mm, which is in line with the code requirements.

The poor soil quality is not enough for the stress requirements of the foundation, so it is not suitable to use natural ground. Considering the calculation of the base processing of the prototype, $f_{spk} = 257.32 \text{ kPa}$ and the characteristic value of the bearing capacity of the composite foundation is considered to be 250 kPa.

3.2.2. Calculation of Rebars

When the rebars of the foundation are determined, the load effect is taken according to the basic combination of the load under the ultimate state of bearing capacity. The bottom rebars of the baseplate are calculated according to the two working conditions of the bearing capacity of the one-way plate and the minimum rebar ratio of the one-way plate. The baseplate's bending capacity is calculated according to the fixed one-way plate at both ends, and the plate strip with a width of 1 m in the middle is calculated. According to the *Static Calculation Handbook for Practical Structure [36]*, the maximum net reaction force at the base edge P_{jmax} is calculated as 163.98 kPa according to Formula (11).

Formula (12) calculates the net reaction force at the bottom of the foundation $P_{1'}$, which equals 121.52 kPa. The net reaction width of the foundation bottom surface a_c' is 12.42 m, the circumferential bending moment of the bottom surface is 37.74 kN·m, the circumferential reinforcement area of the bottom surface of the baseplate is 285.40 mm² (structural reinforcement), and the radial reinforcement area of the bottom surface of the baseplate is 600 mm² (minimum reinforcement). Therefore, the design of the reinforcing baseplate bottom circumferential reinforcement is 16@150 (unit length of reinforcement area of 1340 mm²), and the bottom radial reinforcement is 3 roots 16 (unit arc length radial reinforcement area of 603 mm²).

Similarly, the reinforcement calculation of the top surface of the baseplate is carried out. Under the action of self-weight, the pressure on the tensile side is 99.87 kPa, and the circumferential bending moment of the top surface is 31.02 kN·m. The circumferential reinforcement area of the top surface of the baseplate is 234.24 mm², and the radial reinforcement area of the top surface of the baseplate is 600 mm². Therefore, the circumferential reinforcement of the top surface of the baseplate is 14@150 (unit length of reinforcement

area of 1026 mm²), and the radial reinforcement of the top surface of the bottom surface is 3 roots 16 (unit arc length radial reinforcement area of 603 mm²).

$$P_{j\max} = P_{k\max} - \frac{G_k}{A}, \quad (11)$$

$$P'_1 = \frac{a'_c - \frac{D}{2}(1 - \cos \frac{\pi}{n}) - h}{a'_c} P_{j\max}, \quad (12)$$

The rib beam reinforcement is divided into a bottom and top reinforcement calculation, rib beam oblique section shear, and a rib beam bending bearing capacity calculation. The height of the beam at the root of the ribbed beam is 3500 mm, the beam width is 250 mm, and the reinforcement area at the bottom of the ribbed beam is 6141.08 mm². Therefore, the reinforcement at the bottom of the ribbed beam is designed to be 9 roots 32, and the reinforcement area is 7238 mm². The reinforcement area at the top of the ribbed beam is 3129.22 mm², so the reinforcement at the top of the ribbed beam is designed to be 4 roots 32, and the reinforcement area is 3217 mm². It is calculated that the shear force at the root of the ribbed beam is 1474.69 kN, the stirrup of the ribbed beam is 12@200, and the design value of the shear capacity is 8166.37 kN, which is greater than the shear force at the root of the ribbed beam. The bending capacity is 7531.77 kN·m, and the shear capacity of the inclined section is 2465.97 kN, both of which are greater than the design value, so the reinforcement is reasonable and meets the requirements.

4. Structural FEM Analysis

4.1. Finite Element Model

We used the finite element software ABAQUS (<https://www.3ds.com/products/simulia/abaqus>) to establish the prototype finite element model including foundation, rebars, and soil. The whole finite element model is shown in Figure 8. Specific details and dimensions are shown in Figure 4: the diameter of the base is 21.6 m, the diameter of the pillar is 6.8 m, and the thicknesses of the baseplate and rib beams are 0.4 m and 0.25 m.

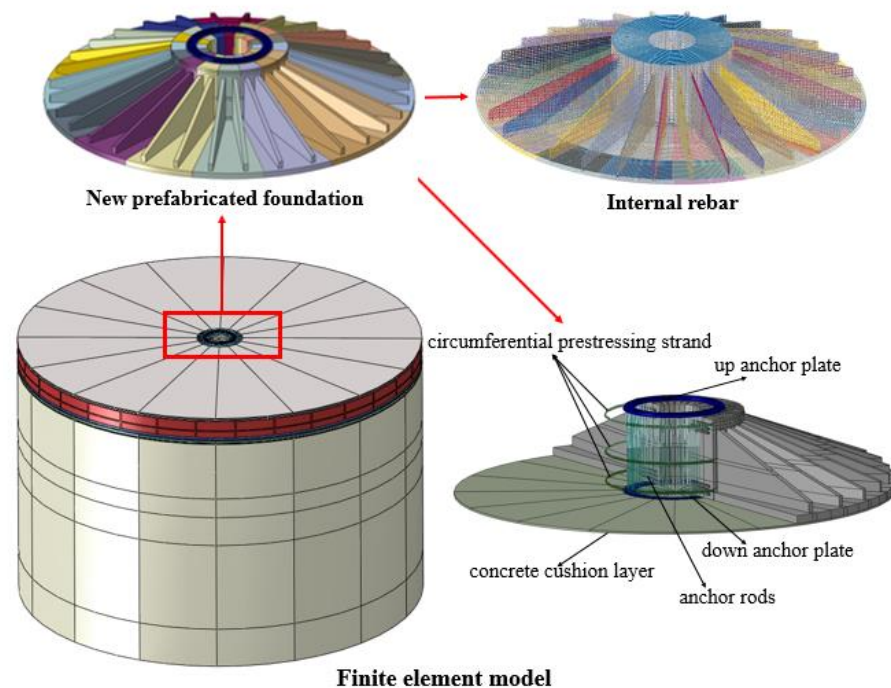


Figure 8. Overall finite element model.

The foundation is simulated using Concrete Damaged Plasticity (CDP), and the foundation and soil are meshed using an eight-node reduced integral solid element (C3D8R). The foundation material is C40 concrete and the cushion material is C20 concrete. The steel structure and rebars are simulated using a linear elastic model, and the solid element (C3D8R) and the truss element (T3D2) are used for meshing. The meshing is shown in Figure 9, with a total number of 151,507 elements, 40,665 linear hexahedral elements of type C3D8R, and 110,842 linear line elements of type T3D2.

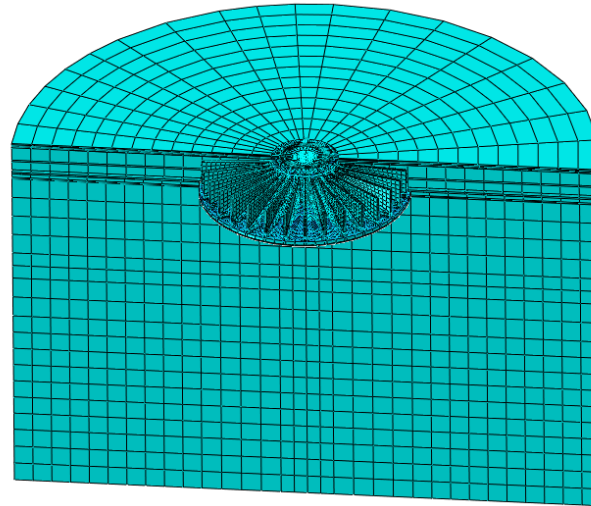


Figure 9. The meshing of the finite element model.

The physical parameters of the soil in the actual project are taken, and the ideal elastic–plastic constitutive model based on the Mohr–Coulomb yield criterion is used for simulation. The soil parameters are shown in Table 4. The diameter of the soil body is 60 m and the height is 40 m. The bottom surface of the soil is fully fixed ($U_1 = U_2 = U_3 = UR_1 = UR_2 = UR_3 = 0$) and the side surfaces are horizontally restrained ($U_1 = U_2 = UR_3 = 0$).

Table 4. Soil parameters.

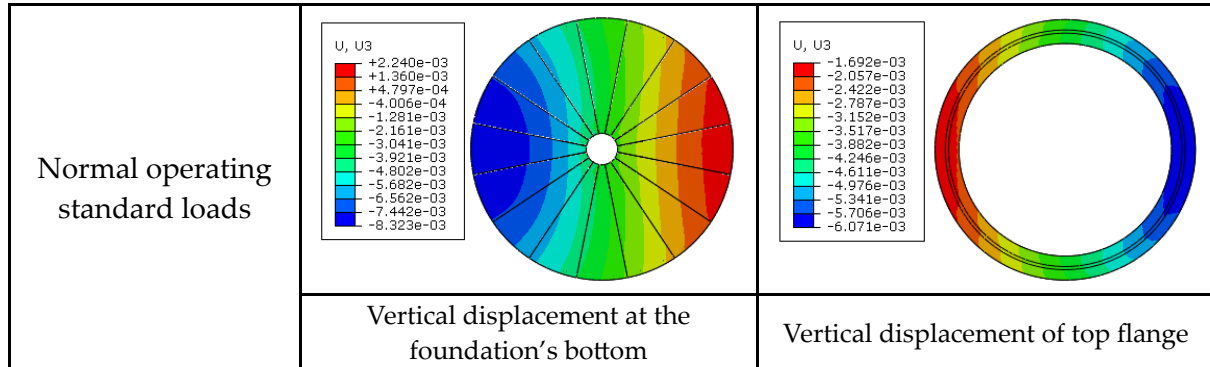
Layer of Soil	Soil Height (m)	Density		Elastic		Mohr Coulomb Plasticity	
		Mass Density ($\text{kg}\cdot\text{m}^{-3}$)	Young's Modulus (MPa)	Poisson's Ratio	Friction Angle ($^{\circ}$)	Plasticity Angle ($^{\circ}$)	
1	4	1420	26.70	0.35	30.30	0.1	
2	9	2000	77.85	0.35	49.80	0.1	
3	3	2000	90.45	0.35	48.45	0.1	
4	4.5	1540	44.40	0.35	27.60	0.1	
5	13.5	1594	48.72	0.35	29.52	0.1	
6	6	1668	54.11	0.35	28.70	0.1	

In the actual construction process, it is necessary to grout the pillar part. In order to make the finite element analysis more consistent with the actual situation, tie contact is used between the pillars in the finite element model, and no contact is set between the baseplates. Surface-to-surface contact is used between the soil and the foundation cushion to simulate the interaction. The friction coefficient is 0.35.

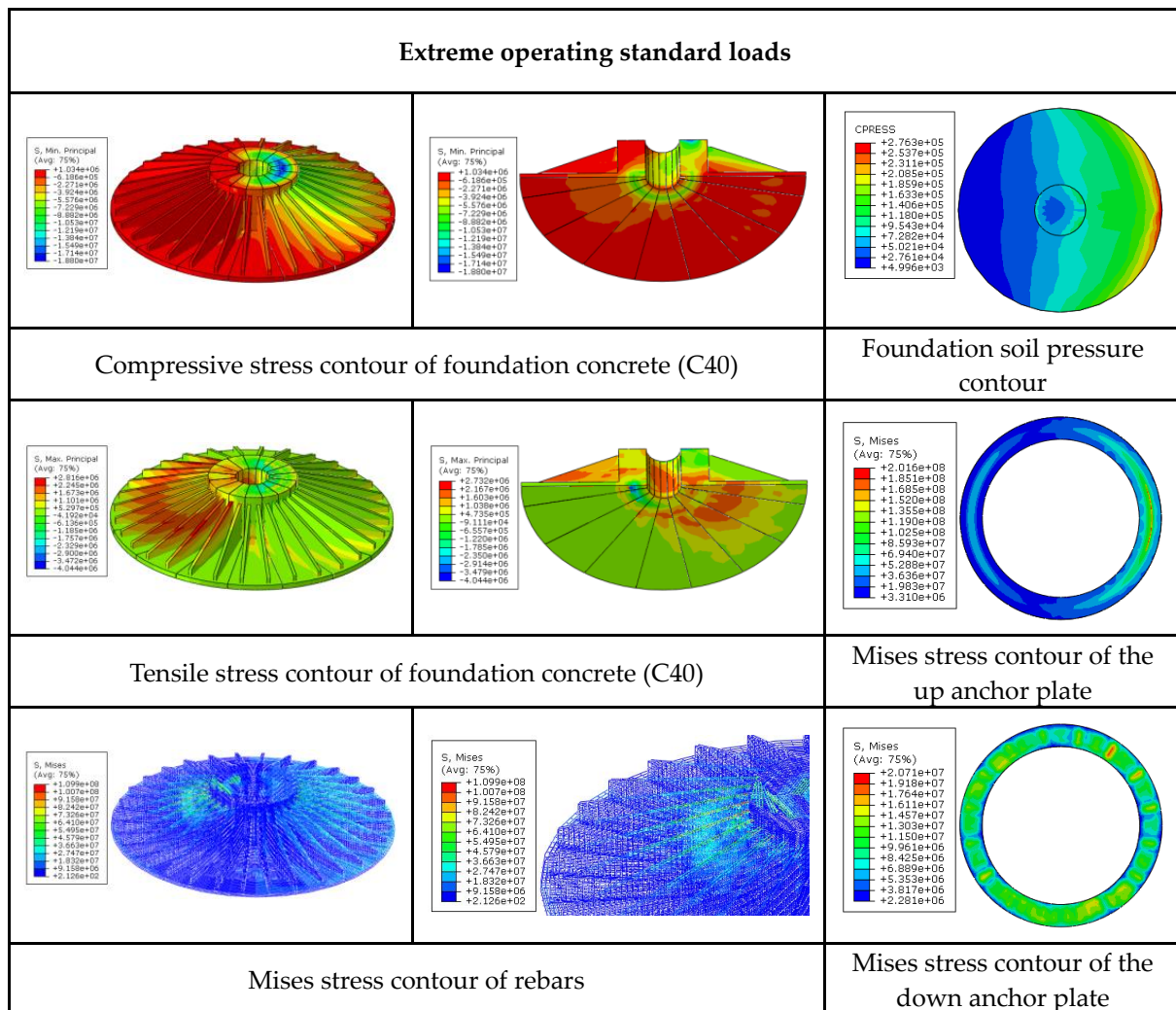
4.2. Structural Finite Element Analysis

Foundation structure forces under normal standard loads and extreme operating conditions were calculated. The results are shown in Figure 10. From Figure 10a, it can be

seen that under normal operating conditions, the vertical displacement at the bottom of the prototype foundation and the vertical displacement at the top flange are 10.562 mm and 4.379 mm, and the tilt rates are 0.49‰ and 0.89‰. The allowable value of the tilt rate of the onshore wind turbine foundation with $90 < H \leq 120$ m is 3‰, so the tilt rate of the new prefabricated foundation meets the requirements.



(a)



(b)

Figure 10. The stress contour of the prototype foundation. (a) Normal operation standard loads calculation results (units: m). (b) Extreme operation standard loads calculation result (units: Pa).

Figure 10b shows that under extreme operating conditions, the maximum compressive stress of the foundation is 18.80 MPa, which is less than the design value of C40 concrete compressive strength $f_{ck} = 19.1$ MPa and meets the requirements. The maximum tensile stress of the foundation is 2.82 MPa, which is greater than the design value of C40 concrete tensile strength of C40 concrete $f_{tk} = 2.39$ MPa. Therefore, the crack width is further checked. The formula is:

$$\omega_{\max} = \alpha_{cr} \psi \frac{\sigma_s}{E_s} \left(1.9c_s + 0.08 \frac{d_{eq}}{\rho_{te}} \right) \quad (13)$$

The calculated maximum crack width at the top of the beam ω_{\max} is 0.029 mm, which is less than 0.2 mm, meeting the requirement.

From Figure 10, it is clear that the maximum stress on the compression side is located at the intersection of the grout layer and the pillar. This is because the annular grouting layer bears the wind turbine load transmitted from the up anchor plate, resulting in a relatively concentrated stress at this position. In addition, the compressive stress of the concrete on the compression side is evenly spread across the adjacent foundation blocks. This shows that the new preassembled foundation structure is still a whole structure and that the foundation blocks have not moved or separated. In the new prefabricated foundation, in addition to the large compressive stress at the junction of the grouting layer and the pillar, there is also a large compressive stress at the junction of the column and the rib beam, which is manifested as the trend of diffusion along the junction of the pillar and the rib beam to the baseplate. It is further explained that the stress distribution of the foundation structure is relatively uniform and reasonable, and there is no obvious local stress concentration or abnormal situation. Such stress distribution characteristics ensure the stability and safety of the infrastructure, providing reliable support for the normal operation of the wind turbine.

The stress range of the up and down anchor plates is 2.28~201.60 MPa, which meets the requirements. The maximum soil pressure at the bottom of the foundation is 276.30 kPa, and the edge of the bottom plate to the main wind direction is a large area of soil pressure. The theoretical calculation of the maximum soil pressure of the foundation is 257.32 kPa, with an error of 6.97%.

The stress range of the main rebars in the foundation is 9.16~109.90 MPa. The stress contour of the rebars in each part of the foundation is shown in Figure 11. It can be seen from Figure 8 that the overall stress distribution of the new prefabricated foundation structure is uniform and reasonable, and it is symmetrically distributed along the loading direction. The stress of foundation rebars diffuses uniformly along the loading direction and is similar to the stress distribution of concrete. The maximum stress positions of the annular and radial rebars in the up and down layers of the baseplate are relatively close, and the rebars stress are 39.26 MPa and 39.22 MPa, which indicates that the reinforcement design of the baseplate is reasonable, and the load transfer law is good. In the prototype structure of the new prefabricated foundation, the stress is relatively concentrated at the junction of the pillar and rib beam. Therefore, in the later indoor scale model test, we should pay attention to this position to ensure the stability and safety of this area.

From the above finite element analysis, it is evident that the design of the new prefabricated foundation structure is reasonable, and it can be put into production and application.

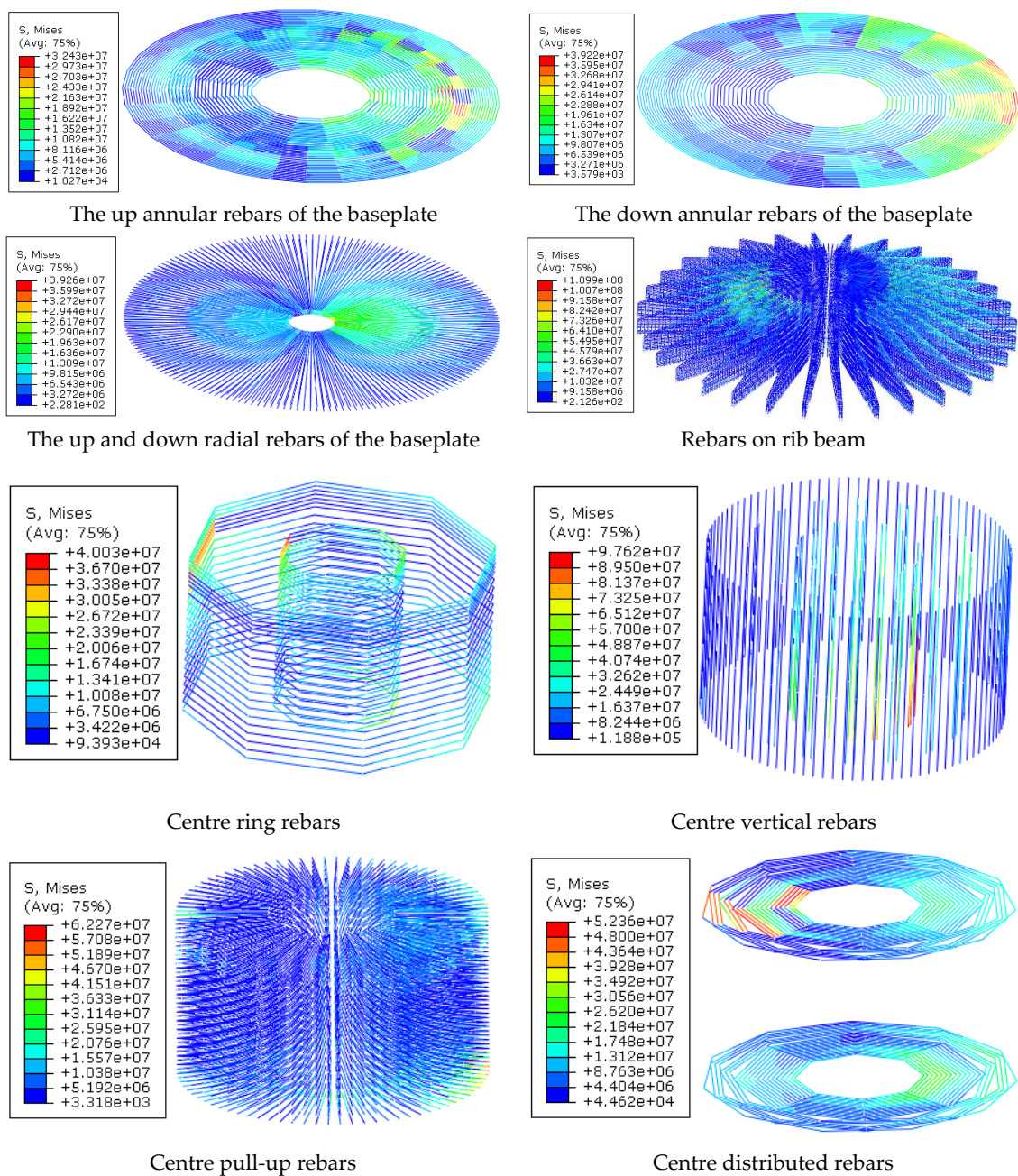


Figure 11. The stress contour of the rebars in the foundation (units: Pa).

5. Conclusions

In this paper, the rationality and superiority of the designed new prefabricated foundation are verified through theoretical calculations and finite element analysis, and the force characteristics of the new prefabricated foundation are also studied.

- (1) A new type of prefabricated foundation for onshore wind turbines is proposed. The new prefabricated foundation consists of 16 prefabricated blocks. Compared with the extended foundation at the same position, the concrete amount is reduced by 30.00%, and the rebars amount is reduced by 34.69%, significantly reducing the amount of reinforcing steel and concrete. At the same time, the new prefabricated foundation blocks can be precast in bulk indoors by means of a precast concrete plant, which can significantly reduce costs and ensure quality. The new prefabricated foundation combines the prefabricated girder slab foundation and the table pillar section as a

- whole, reducing the number and type of prefabricated components while improving construction efficiency.
- (2) Based on the specification, the new prefabricated foundation was inspected and calculated. The calculation results indicate that the foundation's stress and reinforcement meet the specification requirements. Additionally, structural calculations based on several specifications show that the new prefabricated foundation meets the design requirements of the specifications in terms of bearing capacity, stability against overturning, stability against sliding, settlement, and other factors. The new prefabricated foundation is stable and safe enough.
 - (3) Based on the finite element analysis software ABAQUS, the rebars stress, concrete stress, and foundation inclination rate of the new prefabricated foundation were analyzed. Through the analysis of the stress distribution of foundation concrete and rebars, it can be found that the stress distribution is reasonable and uniform, and the load transfer is fine. The maximum stress of the rebars and concrete does not exceed the specification limit, and the concrete does not crack.
 - (4) The tilt rates of the bottom flange of the foundation and the bottom flange of the fan are 0.49‰ and 0.89‰, respectively, which do not exceed the normative permissible value of 3‰, and the tilt rate of the foundation meets the specification requirements. The design of the new prefabricated foundation is reasonable. It meets the specification requirements and the actual bearing demand, and it has great mechanical properties and stability. It provides theoretical support for subsequent measurement of indoor experiments and field construction.

Author Contributions: Conceptualization, J.L. and H.H.; methodology, X.L., H.W. and Y.G.; software, X.L., H.H. and L.Z.; investigation, Y.D. and X.W.; resources, C.Z.; writing—original draft preparation, X.L. and Y.G.; writing—review and editing, Y.G., L.Z. and H.W.; visualization, X.W. and C.Z.; project administration, H.W.; funding acquisition, H.H. and L.Z. All authors have read and agreed to the published version of the manuscript.

Funding: This research was funded by the Fundamental Research Funds for the China Huaneng Group (HNKJ21-H37).

Data Availability Statement: Data are contained within the article.

Acknowledgments: The authors thank all the people who have supported this research.

Conflicts of Interest: Authors Huageng Hao and Liying Zhang were employed by the company China Huaneng Group Clean Energy Research Institute Co., Ltd. Author Yanyi Du was employed by the company Huaneng Longdong Energy Co., Ltd. Author Xianwen Wang was employed by the company Huaneng Jilin Power Generation Co., Ltd. The remaining authors declare that the research was conducted in the absence of any commercial or financial relationships that could be construed as a potential conflict of interest.

Abbreviations

The following symbols are used in this paper:

P_{kmax}	is the maximum pressure value at the bottom edge of the foundation under the standard combination of load effect.
P_{kmin}	is the minimum pressure value at the bottom edge of the foundation under the standard combination of load effect.
N_k	is the vertical load transmitted from the superstructure to the top surface of the foundation.
M_k	is the resultant moment value of the superstructure to the top surface of the foundation.
G_k	is the weight of foundation and overlying soil.
W	is the resistance moment of the base surface.
A	is the base area.
ξ	is the maximum pressure coefficient of the foundation's bottom surface.
R	is the radius of the foundation's bottom surface.

F_R	is the anti-sliding force under the basic combination of load effect.
μ	is the friction coefficient between the foundation bottom and foundation.
F_s	is the design value of sliding force under the basic combination of load effect.
γ_0	is the structural importance coefficient, and the structural safety level is 1.1 for the first level and 1.0 for the second level.
γ_d	is the structural coefficient, and 1.3 is taken in the calculation of anti-sliding stability and 1.6 is taken in the calculation of anti-overturning stability.
M_R	is the anti-overturning moment under the basic combination of load effect.
M_S	is the design value of overturning moment under the basic combination of load effect.
d	is the diameter of the new prefabricated foundation.
s	is the final settlement value of the foundation.
s'	is the foundation settlement value calculated using the layered sum method.
ψ_s	is an empirical coefficient for settlement calculations.
n	is the number of soil layers divided within the depth of the foundation settlement calculation.
E_{si}	is the compression modulus of the soil in layer i below the base of the extended foundation.
P_{0k}	is the additional stress at the base of the extended foundation for the standard combination of load effects.
z_i, z_{i-1}	are the distances from the base of the extended foundation to the base of the $i, i-1$ layer of soil.
$\bar{\alpha}_i, \bar{\alpha}_{i-1}$	are the average additional stress coefficients in the range from the calculation point at the base of the extended foundation to the base of the i and $i-1$ layer of soil.
f_{spk}	is the eigenvalue of foundation bearing capacity.
P_{jmax}	is the maximum net reaction force at the base edge.
P_1'	is the net reaction force at the bottom of the foundation to calculate the strip.
a_c	is the width of the net reaction force on the foundation bottom surface.
ω_{max}	is the maximum crack width of the foundation slab
α_{cr}	is the member force characteristic factor
ψ	is the coefficient of strain inhomogeneity of the longitudinal tensile reinforcement between cracks
σ_s	is the stress in the longitudinal tensile plain reinforcement of reinforced concrete members calculated on the basis of quasi-permanent combinations of loads/equivalent stress in the longitudinal tensile reinforcement of prestressed concrete members calculated on the basis of standard combinations.
E_s	is the modulus of elasticity of the reinforcement
c_s	is the distance from the outer edge of the outermost longitudinal tension reinforcement to the base plate of the tension zone
d_{eq}	is the equivalent diameter of the longitudinal reinforcement in the tension zone
ρ_{te}	is the reinforcement ratio of longitudinal tensile reinforcement based on the effective tensile concrete section area.

References

- Li, C.; Mogollón, J.M.; Tukker, A.; Steubing, B. Environmental Impacts of Global Offshore Wind Energy Development until 2040. *Environ. Sci. Technol.* **2022**, *56*, 11567–11577. [CrossRef] [PubMed]
- Guo, Y.; Wang, H.; Lian, J. Review of Integrated Installation Technologies for Offshore Wind Turbines: Current Progress and Future Development Trends. *Energy Convers. Manag.* **2022**, *255*, 115319. [CrossRef]
- Gielen, D.; Gorini, R.; Wagner, N.; Leme, R.; Gutierrez, L.; Prakash, G.; Asmelash, E.; Janeiro, L.; Gallina, G.; Vale, G.; et al. Global Energy Transformation: A Roadmap to 2050. 2019. Available online: <https://www.h2knowledgecentre.com/content/researchpaper1605> (accessed on 15 October 2023).
- Yang, T.; Pan, Y.; Yang, Y.; Lin, M.; Qin, B.; Xu, P.; Huang, Z. CO₂ Emissions in China's Building Sector through 2050: A Scenario Analysis Based on a Bottom-up Model. *Energy* **2017**, *128*, 208–223. [CrossRef]
- Borthwick, A.G.L. Marine Renewable Energy Seascape. *Engineering* **2016**, *2*, 69–78. [CrossRef]
- Global Wind Energy Council. *GWEC Global Wind Report 2023*; Global Wind Energy Council: Sao Paulo, Brazil, 2023.
- Duffy, A.; Hand, M.; Wiser, R.; Lantz, E.; Dalla Riva, A.; Berkhout, V.; Stenkvist, M.; Weir, D.; Lacal-Arántegui, R. Land-Based Wind Energy Cost Trends in Germany, Denmark, Ireland, Norway, Sweden and the United States. *Appl. Energy* **2020**, *277*, 114777. [CrossRef]
- Faber, T. Tower and Foundation. In *Wind Power Technology: An Introduction*; Springer International Publishing: Cham, Switzerland, 2023; pp. 291–318.

9. Al-Shetwi, A.Q. Sustainable Development of Renewable Energy Integrated Power Sector: Trends, Environmental Impacts, and Recent Challenges. *Sci. Total Environ.* **2022**, *822*, 153645. [CrossRef] [PubMed]
10. Bradford, T. *Solar Revolution: The Economic Transformation of the Global Energy Industry*; MIT Press: Cambridge, MA, USA, 2008.
11. Zohuri, B. Navigating the Global Energy Landscape Balancing Growth, Demand, and Sustainability. *J. Mat. Sci. Appl. Eng.* **2023**, *2*, 7.
12. Bai, J.; Wang, R.; Wang, Y.; Yang, Q. A review of onshore wind turbine prefabricated foundation structures. *J. Civ. Environ. Eng.* **2023**, 1–15.
13. Shang, Z.; Wang, F.; Yang, X. The Efficiency of the Chinese Prefabricated Building Industry and Its Influencing Factors: An Empirical Study. *Sustainability* **2022**, *14*, 10695. [CrossRef]
14. Song, H.; Cong, O.; Hao, H.; Xu, Y. Research on mechanical properties of prefabricated foundation of wind turbine generators. *Bulid. Struct.* **2018**, *48*, 96–100. [CrossRef]
15. Diógenes, J.R.F.; Claro, J.; Rodrigues, J.C.; Loureiro, M.V. Barriers to Onshore Wind Energy Implementation: A Systematic Review. *Energy Res. Soc. Sci.* **2020**, *60*, 101337. [CrossRef]
16. El-Abidi, K.M.A.; Ghazali, F.E.M. Motivations and Limitations of Prefabricated Building: An Overview. *Appl. Mech. Mater.* **2015**, *802*, 668–675. [CrossRef]
17. Wang, W.; Gao, Y.; Wang, Z.; Zhang, L.; An, Z.; Shao, S. An Experimental Study on Plate Splicing of Prefabricated Plate Foundation. *Buildings* **2023**, *13*, 2114. [CrossRef]
18. De Lana, J.A.; Magalhães, P.A.A., Jr.; Magalhães, C.A.; Magalhães, A.L.M.A.; De Andrade Junior, A.C.; De Barros Ribeiro, M.S. Behavior Study of Prestressed Concrete Wind-Turbine Tower in Circular Cross-Section. *Eng. Struct.* **2021**, *227*, 111403. [CrossRef]
19. Zhang, Y. Study on Application of Prefabricated Steel Foundation in Wind Power Tower. Master's Thesis, Tongji University, Shanghai, China, 2018.
20. Chen, Z.; Li, H.; Chen, A.; Yu, Y.; Wang, H. Research on Pretensioned Modular Frame Test and Simulations. *Eng. Struct.* **2017**, *151*, 774–787. [CrossRef]
21. Adrian, C.; Doug, K. Tower Foundation with Concrete Box Girder Beams. U.S. Patent 10982406, 20 April 2021.
22. Marta, C.D.; Rüdiger, M.; Ali Mohammadi, M. Mold Part Set for Wind Turbine Ground Foundation and Wind Turbine Ground Foundation. WO2022174912A1, 25 August 2022.
23. Anker Foundations. “Wind Turbine Foundations” [EB/OL]. Available online: <https://www.anker-foundations.com/en/wind-turbine-foundation/> (accessed on 1 October 2023).
24. Wu, X.; Li, W.; Liu, W. Bearing Platform Unit and Modular Assembly Type Wind Power Extended Foundation with Same. CN217630065U, 21 October 2022.
25. Velasquez, R.A.; Morgan, K.B.; Krause, D.J. Challenges Evaluating Performance of Innovative Wind Turbine Foundation via 3D Numerical Modeling. In Proceedings of the Geo-Congress 2020, Minneapolis, MN, USA, 25–28 February 2020; American Society of Civil Engineers: Minneapolis, MN, USA, 2020; pp. 325–333.
26. Krause, D.E. Beam and Pile Anchor Foundation for Towers. U.S. Patent 20180187389, 5 July 2018.
27. Ma, R.; He, M. Prestress Anchor Bolt Prefabricated Assembled Cylinder Blower Base. CN201411706Y, 24 February 2010.
28. Tang, T. Study on Precast Prestressed Tubular Foundation of Wind Turbine. Master's Thesis, Tongji University, Shanghai, China, 2009.
29. Serna, G.-C.; José, S. Foundations System for Towers and Method for Installing the Foundations System for Towers. U.S. Patent 20170152641, 1 June 2017.
30. Norvell, C. Structural Design Issues of “Hexapod” Foundations for Wind Turbine Towers. Master's Thesis, Portland State University, Portland, OR, USA, 2016.
31. Guo, Y.; Zhang, P.; Ding, H.; Le, C. Design and Verification of the Loading System and Boundary Conditions for Wind Turbine Foundation Model Experiment. *Renew. Energy* **2021**, *172*, 16–33. [CrossRef]
32. Mehra, S.; Trivedi, A. Pile Groups Subjected to Axial and Torsional Loads in Flow-Controlled Geomaterial. *Int. J. Geomech.* **2021**, *21*, 04021002. [CrossRef]
33. NB/T 10311-2019; Code for Design of Wind Turbine Foundations for Onshore Wind Power Projects. China Water Power Press: Beijing, China, 2020.
34. Zhang, L. Study on Numerical Simulation and Optimal Design of Wind Turbine Foundation. Master's Thesis, Tianjin University, Tianjin, China, 2009.
35. GB 50007-2011; Code for Design of Building Foundation. China Architecture & Building Press: Beijing, China, 2012.
36. Guo, Z.; Zhang, S. *Static Calculation Handbook for Practical Structure*; China Machine Press: Beijing, China, 2009; Volume 4, pp. 320–322.

Disclaimer/Publisher's Note: The statements, opinions and data contained in all publications are solely those of the individual author(s) and contributor(s) and not of MDPI and/or the editor(s). MDPI and/or the editor(s) disclaim responsibility for any injury to people or property resulting from any ideas, methods, instructions or products referred to in the content.